Decreased Blood Flow with Increased Metabolic Activity: A Novel Sign of Pancreatic Tumor Aggressiveness

Gaber Komar,[1] Saila Kauhanen,[1,2] Kaisa Liukko,[1] Marko Seppänen,[1] Sami Kajander,[1] Jari Ovaska,[2] Pirjo Nuutila,[1,3] and Heikki Minn[1,4]

Abstract

Purpose: To study blood flow (BF) and metabolism in normal pancreas and in different pancreatic lesions. We then determined the effect of these biomarkers on outcome in patients with pancreatic cancer.

Experimental Design: Oxygen-15–labeled water and fluorodeoxyglucose positron emission tomography/computed tomography scans were used in 26 patients with a suspicion of pancreatic cancer to measure pancreatic BF and metabolism. In addition, the ratio of standardized uptake value to BF (SUV/BF) was calculated. Patients were divided into three groups: patients with a finding of normal pancreas ($n = 7$), benign lesions ($n = 8$), and malignant tumors ($n = 11$).

Results: Patients with benign and malignant pancreatic tumors had decreased BF of the lesion by 48% and 60%, respectively, compared with patients with normal pancreatic tissue. SUV_{max} was 3-fold higher in malignant tumors compared with both benign lesions and normal pancreas ($P < 0.05$). In contrast, the SUV_{max} of patients with benign lesions and normal pancreas did not differ. The SUV/BF ratio was significantly higher in malignant lesions than in benign lesions or in patients with normal pancreas ($P < 0.05$). In patients with cancer, high SUV/BF ratio was a stronger predictor of poor survival compared with high metabolism or lower-than-normal pancreatic BF.

Conclusions: BF in pancreatic cancer is significantly reduced compared with the normal pancreas, which may in part explain the poor success of both radiotherapy and chemotherapy. We suggest that the composite measurement of BF and metabolism in pancreatic cancer could serve as a novel tool in the planning of treatments targeting vasculature. (Clin Cancer Res 2009;15(17):5511–7)

Despite intensive efforts, the prognosis for patients with pancreatic malignancies, and in particular, pancreatic adenocarcinoma, remains very grave (1), with radical surgery increasing 5-year survival from <4% to only 10% to 20% (2). The benefits of systemic chemotherapy combined with radiation are even more limited. Although gemcitabine and fluorouracil show modest activity, there is much debate on their role in the initial treatment of inoperable lesions (3). The reason for relative treatment resistance could be the low perfusion found in pancreatic malignant lesions compared with the normal pancreas, already indicated by early angiographic studies (4). The angiogenesis of tumors is important in predicting the growth and metastasis of pancreatic cancer. Therefore, drugs targeting the inhibition of oncogenic signaling pathways to block angiogenesis have recently been developed (5). The fact that antiangiogenic drugs have not consistently provided significant benefits in pancreatic cancer (6) could be due to the large variability in perfusion found in untreated lesions. Failure to observe normalization of the vasculature in responding patients may be due to the insensitivity of standard (morphologic) imaging methods to measure functional changes.

Due to the inaccessibility of the organ and the lack of an established noninvasive method, quantification of pancreatic perfusion presents a challenge in routine clinical practice. Several attempts to solve this problem have been undertaken with the help of different imaging techniques. Among these are angiography (4), dynamic contrast enhanced (DCE) computed tomography (CT; refs. 7, 8), ultrasonography (9), magnetic resonance imaging (10), and positron emission tomography (PET; ref. 11). A problem common to all these methods, when used in humans, is the lack of an accepted reference standard. This also partly explains why the perfusion of normal pancreatic tissue measured in these studies has varied substantially.

Authors' Affiliations: [1]Turku PET Centre, [2]Department of Surgery, Turku University Central Hospital, Departments of [3]Medicine and [4]Oncology and Radiotherapy, University of Turku, Turku, Finland

Received 2/17/09; revised 5/22/09; accepted 5/27/09; published OnlineFirst 8/25/09.

Grant support: EU FP6 Commission "Biocare" Molecular Imaging for Biologically Optimized Cancer Therapy (no. 505785) and Turku University Hospital (no. 13018) "Turku University Foundation." Conducted within the "Turku Centre of Excellence in Molecular Imaging in Cardiovascular and Metabolic Research."

The costs of publication of this article were defrayed in part by the payment of page charges. This article must therefore be hereby marked *advertisement* in accordance with 18 U.S.C. Section 1734 solely to indicate this fact.

Note: G. Komar and S. Kauhanen contributed equally to this work.

Requests for reprints: Gaber Komar, Turku PET Centre, Kiinamyllynkatu 4-8, 20521 Turku, Finland. Phone: 358-2313-2772; Fax: 358-2231-8191; E-mail: gaber.komar@utu.fi.

doi:10.1158/1078-0432.CCR-09-0414

Translational Relevance

With an increasing number of new drugs targeting specific molecular pathways, it is becoming clear that careful selection of patients prior to treatment is crucial for the success and cost-effectiveness of such targeted therapies. The aim of this study was to measure blood flow (BF) and metabolism in normal pancreas and in different pancreatic lesions using positron emission tomography/computed tomography, and to determine the prognostic values of these variables. We found decreased BF in both malignant and benign lesions compared with normal pancreas, whereas increased metabolic activity was seen only in malignant lesions. The ratio of metabolism to BF was an important prognostic variable supporting that high metabolism combined with low perfusion is linked to an aggressive phenotype. Our initial findings may in part explain the general resistance of pancreatic cancer to oncologic treatments, and suggest the inclusion of combined perfusion and metabolism imaging in clinical trials in which antiangiogenic treatment is evaluated.

Currently, the most reliable noninvasive method to quantify perfusion is PET using oxygen-15–labeled water ($[^{15}O]H_2O$; ref. 12). This method has previously been extensively tested and validated for several tissue and tumor types among others also in our center (13, 14). PET imaging of perfusion has typically indicated higher values in tumors compared with the parent tissue (15). On the other hand, only one study has attempted to measure pancreatic perfusion using $[^{15}O]H_2O$ PET and a semiquantitative approach with a finding of decreased blood flow (BF) among pancreatic tumors (11). This pilot study was done with a stand-alone PET scanner without the added benefit of the precise anatomic reference provided by CT and the compensation of the suboptimal spatial resolution inherent in PET images. Second, the relationship between tumor perfusion and its metabolic activity studied with fluorodeoxyglucose ($[^{18}F]$FDG) PET/CT imaging may be important for treatment monitoring and for prognosis (16).

In this context, we attempted to noninvasively quantify the BF and metabolic activity of pancreatic tumors using $[^{15}O]H_2O$ and $[^{18}F]$FDG PET/CT imaging. We compared the findings in malignant tumors to those in normal pancreatic tissue and benign lesions, and further assessed the effects of these functional variables on the survival of patients with confirmed cancer.

Materials and Methods

Patient population. Twenty-six consecutive patients (14 males and 12 females, ages 64.8 ± 12.5 y) with clinical suspicion of pancreatic malignancy were, prior to any treatment, prospectively enrolled in the study between September 2006 and October 2007. Criteria for enrollment in PET/CT imaging was a suspicion of malignant biliary stricture at endoscopic retrograde cholangiopancreatography (n = 15), or a suspicious pancreatic lesion on ultrasonography or CT in a referring center (n = 11). Validation of diagnosis was based on the findings at operation with biopsy (n = 11), operation without biopsy (n = 4), percutaneous/cytologic brush biopsy (n = 2), autopsy (n = 1), or follow-up of a median of 20.1 mo (range, 16-27 mo; n = 8). Patients were divided into three groups as follows: group A, no anatomic tumor (n = 7); group B, benign lesion (n = 8); and group C, malignant pancreatic tumor (n = 11). The study was conducted in accordance with the Declaration of Helsinki, and the study protocol was approved by the ethics committee of the Hospital District of Southwest Finland and the Finnish National Agency for Medicine. All patients gave their written informed consent before participating in the study.

PET/CT device. All data were acquired on a Discovery VCT PET/CT scanner (General Electric Medical Systems) which combines a helical 64-slice CT scanner and a bismuth germanate oxide block PET tomography. The PET scanner part consists of 13,440 bismuth germanate oxide crystals arranged in 24 rings, yielding 47 transverse slices spaced axially by 3.27 mm. The PET imaging field of view was 70 cm in diameter and 15.7 cm in axial length. Attenuation correction was done using a low-dose ultra-fast CT protocol (80 mAs, 140 kV, 0.3 mSv per field of view). The voxel size of the PET image is 3.5 × 3.5 × 3.27 mm. $[^{18}F]$FDG images were reconstructed using two iterations and 28 subsets with a 6.0 mm full-width half-maximum postfilter and a fully three-dimensional maximum likelihood ordered subset expectation maximization reconstruction algorithm. Dynamic two-dimensional $[^{15}O]H_2O$ images were reconstructed using two iterations, 20 subsets, a 6.0 mm full-width half-maximum postfilter and a 5.47 mm loop filter. The 128 × 128 matrix size was used in PET images. A detailed description and performance evaluation of the scanner was recently published by Teräs et al. (17).

Scanning protocol. All patients fasted at least 6 h and their plasma glucose (GlcP) levels was measured before the start of the acquisition. Measurement of tumor BF with $[^{15}O]H_2O$ was followed by PET/CT imaging with $[^{18}F]$FDG. Patients were positioned on the tomography couch in supine position, arms alongside the body. The study started with CT imaging for attenuation correction followed by a bolus injection of $[^{15}O]H_2O$ (mean dose, 1,100 ± 81 MBq; range, 960-1,280 MBq) and an immediate dynamic emission image acquisition of 6 min (26 frames; ref. 18). After this, the patient was removed from the scanner. After the injection of $[^{18}F]$FDG (mean dose, 367 ± 17 MBq; range, 316-386 MBq), the image was acquired according to a standard diagnostic scanning protocol 57 ± 5 (range, 49-70) min postinjection.

Synthesis of $[^{15}O]H_2O$ and $[^{18}F]$FDG. A low-energy deuteron accelerator Cyclone 3 (IBA Molecular) was used for the production of ^{15}O. To synthesize radiowater for BF imaging, a diffusion membrane technique in a constantly working water module was applied (Radio Water Generator). An online radioactivity recording of products was done for each examination with a low-voltage ionization chamber. $[^{18}F]$FDG was synthesized from mannosyl triflate using a nucleophilic method. Radiochemical purity exceeded 95% and specific radioactivity was ~74 GBq/μmol at the end of the synthesis.

Calculation of $[^{15}O]H_2O$-perfusion images. BF images were calculated using a linearized one-tissue compartment model (19). Lawson-Hanson nonnegative least squares were used to solve general linear least squares functions. The input time-activity curves (TAC) for $[^{15}O]H_2O$ scans were obtained directly from transaxial PET images using a threshold method to locate the aorta. Suitable planes were selected visually with the help of PET and CT images. The diameter of the aorta in these planes was measured using the CT image and the value was used in the threshold process as well as in the correction of partial volume and spillover effects during extraction. The method of input curve extraction has been recently described and validated (20). After extraction of the pancreatic tissue TAC from the image series and comparison to arterial TAC, no delay was observed in the ascending part of the TAC and no correction was done.

Image analysis. Images were analyzed on a computer using a noncommercial research imaging software (Vinci, Max-Planck-Institut für Neurologische Forschung, Cologne, Germany). Perfusion and $[^{18}F]$FDG values for different tissues were obtained by positioning a round three-plane region-of-interest (ROI) with a diameter of 1 cm (0.77 cm^3) on the area of the lesion with the highest $[^{18}F]$FDG uptake and copied onto the corresponding region in the perfusion image using the CT

image as anatomic reference. This was facilitated by the good coregistration of PET and CT images from the PET/CT scanner.

Calculation of [18F]FDG standardized uptake values. [18F]FDG activity concentration values were corrected for radioactive decay, and standardized uptake value (SUV) was calculated as SUV = activity concentration in a ROI / (injected dose / body mass). The resulting values were normalized to GlcP levels according to the formula SUV × (GlcP/5) (21). Finally, SUV_{max} normalized to GlcP was divided by BF to obtain the SUV/BF ratio. The example of the SUV/BF image (Fig. 1) was calculated by careful realignment of tumors in both images and reslicing. To obtain the resulting ratio image, the individual [18F]FDG SUV voxel values were divided by the BF values of voxels of the same anatomic position in the BF image.

Statistical analysis. Pearson's correlation coefficient was calculated to test the correlation between BF values of different parts of the pancreas. Unpaired Student's *t* test was used to test the difference between SUV_{max}, BF values, and SUV/BF ratio of normal pancreas, benign, and malignant lesions. $P < 0.05$ was considered statistically significant. All statistical analyses were done with StatView (version 5.0; SAS Institute).

Results

BF in the pancreas. In the group of patients without anatomic tumors (group A, $n = 7$), the BF was higher than that in patients with a benign or malignant lesion (Table 1; Fig. 2A). The BFs of the morphologically normal pancreas was similar between head and tail and the average intraindividual variability expressed as coefficient of variation was 31.7%. Three patients had stones in the main biliary duct, one patient had cytologically confirmed benign main biliary duct stricture, and three patients had a normal pancreas on all imaging modalities.

In the group of benign lesions (group B, $n = 8$), a reduction of BF in comparison to group A was observed (Table 1). BF in the nontumoral part of the pancreas was not significantly reduced in comparison to that seen in patients of group A (Fig. 2A). Of the benign lesions, three were located in the head and five in the body/tail region of the pancreas. The BF between the benign lesion and the nontumoral parts of the pancreas showed good correlation despite of the small number of patients ($R = 0.66$, $P = 0.05$). In group B, two patients had a mass-forming pancreatitis, five patients had a benign cystic lesion, and one patient had a pancreatic fibrosis in histologic analysis. The sizes of the benign lesions were 4.6 ± 2.9 cm (range, 2-11 cm).

Group C ($n = 11$) was composed of nine cases of adenocarcinoma and two cases of neuroendocrine tumors (NET; Table 2). All tumors except one were located in the head or the head/body region, and the reference value in these cases was obtained from the tail of the pancreas. The lesion of one patient (no. 7) was located in the body/tail region of the pancreas, and this patient's reference value was obtained from the head of the pancreas. The BF in malignant lesions was significantly lower than in group A ($P < 0.001$), but not significantly lower than in group B (Table 1; Fig. 2A). In the group with cancer, a strong reduction in BF was also observed in the nontumoral part of the pancreas when compared with group A ($P = 0.02$; Fig. 2A). With the exception of patient no. 7, the BF of the malignant tumor showed a high correlation with that of the nontumoral parts of the pancreas ($R = 0.86$; $P < 0.001$). In this patient, whose malignant lesion was located in the body/tail region, the BF of the lesion was as low as that of other tumors in group C (48.9 mL/min/dL), whereas the BF in the head of the pancreas was very high (168.9 mL/min/dL).

Glucose metabolism of tumors. Glucose metabolism was evaluated using SUV_{max}. The average SUV_{max} for normal pancreas was 2.7 ± 1.3 (range, 1.8-5.1). The SUV_{max} for malignant lesions were significantly higher compared with those for normal pancreas ($P = 0.01$) or benign lesions ($P = 0.01$). Instead, SUVs of benign lesions were not significantly different compared with those for normal pancreas (Table 1; Fig. 2B). The GlcP values were 6.7 ± 1.7, 5.6 ± 0.6, and 7.1 ± 1.8 mmol/L for patients with normal pancreas, benign lesions, and malignant lesions, respectively. Only the difference between GlcP values of patients with benign and malignant lesions was statistically significant (group A versus group B, $P = 0.11$; group A versus group C, $P = 0.61$; group B versus group C, $P = 0.03$). To account for this difference, SUV_{max} was normalized to GlcP levels as explained earlier. The GlcP normalization had the strongest effect on the statistical differences between groups A and B (non-GlcP, $P = 0.12$), but had less effect on other values. The time between injection of [18F]FDG and start of imaging did not differ significantly between the three groups (group A, 58.1 ± 5.9 min; group B, 56.5 ± 3.0 min; and group C, 57.2 ± 5.7 min).

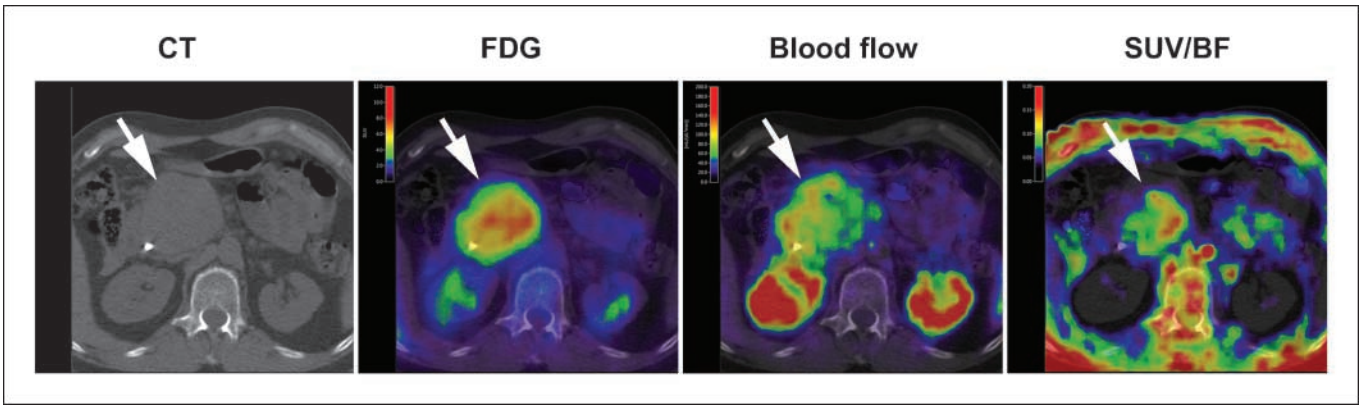

Fig. 1. Combined axial BF and [18F]FDG PET images superimposed on corresponding CT slice in a patient with high-grade neuroendocrine carcinoma. Tumor located in the head of the pancreas (*white arrow*). Note the differential pattern of regional uptake in images representing metabolism ([18F]FDG), BF, and the SUV/BF ratio illustrating the incremental information provided by each functional measurement.

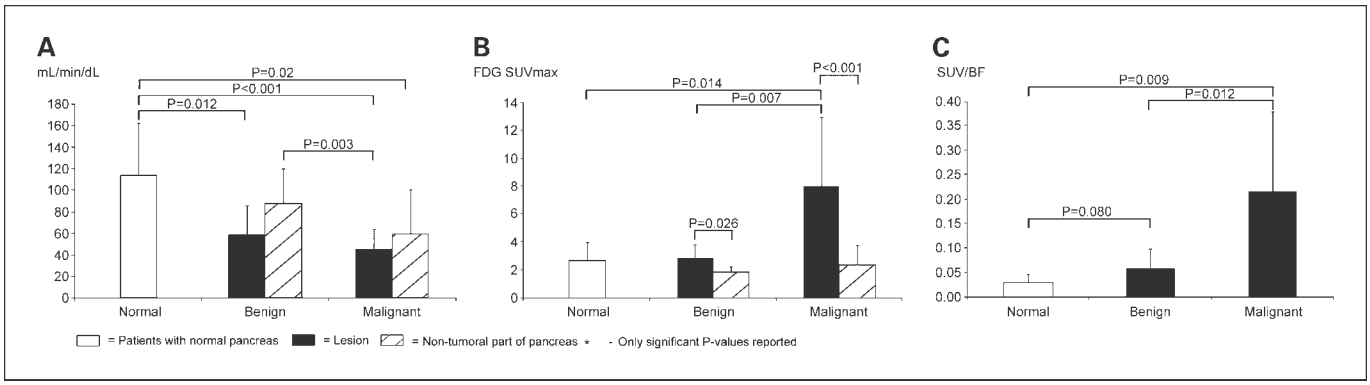

Fig. 2. BF (*A*), metabolism expressed as [^{18}F]FDG SUV_{max} (*B*), and the SUV/BF ratio (*C*) in the three groups of patients.

Correlation of tumor metabolism with BF. As expected, the SUV/BF ratio was significantly different between normal pancreas and malignant lesions ($P = 0.01$), as well as between benign and malignant lesions ($P = 0.01$). By contrast, no difference was observed between SUV/BF of normal pancreas and benign lesions ($P = 0.08$; Fig. 2C). When we plotted the SUV_{max} against the BF values of the same lesion, we observed a clustering of values according to the lesion pathology (Fig. 3). However, there were no significant correlations between [^{18}F]FDG SUV_{max} and BF in any of the three groups.

Correlation of functional measurements with survival. Eleven patients with pancreatic malignancy were followed for at least 13 months after the diagnosis and five of these patients were alive at the time of analysis (Table 2). One patient with low-grade NET died due to complications related to surgery, and therefore we excluded him from the survival analysis. The remaining 10 patients were divided into two groups using survival at 12 months after diagnosis as the cutoff. The SUV_{max} or BF between the groups living shorter or longer than 12 months were not significantly different (SUVmax: 10.6 ± 5.7 versus 6.7 ± 2.7, $P = 0.20$; and BF: 34.2 ± 14.3 versus 55.6 ± 18.7 mL/min/dL; $P = 0.08$, respectively). By contrast, when the SUV/BF ratio was compared between these two groups, a high SUV/BF was associated with poorer prognosis (0.3 ± 1.6 versus 0.1 ± 0.5; $P = 0.02$; Fig. 4).

Discussion

To our knowledge, this is the first prospective study in which BF and metabolism were measured in parallel using [^{15}O]H_2O and [^{18}F]FDG PET/CT in patients presenting with suspicion of pancreatic cancer. We found average BF to be significantly decreased and metabolism significantly increased in malignant pancreatic lesions compared with normal pancreas. Based on our initial findings, we hypothesize that a high ratio of metabolism to BF may predict survival better than either functional measurement alone.

At a time when the possibilities and limitations (22) of new therapeutic agents targeting angiogenic mechanisms of tumors are being recognized, it is becoming obvious that careful classification and selection of patients prior to treatment is necessary for these therapeutic strategies to be successful. This is of particular importance in malignancies with a low likelihood of response, such as pancreatic cancer (6). In this respect, tumor perfusion and metabolism seem to be among the most relevant clinical variables (16, 23). Several methods have been proposed for noninvasive measurement of pancreatic perfusion in humans. Contrast-enhanced ultrasonography (8, 9, 24) and DCE-CT (7) have been used to assess pancreatic perfusion in inflammatory and malignant lesions with encouraging results. Park et al. (25) observed that high perfusion in pancreatic cancer detected on DCE-CT was associated with increased response to chemoradiotherapy. Also, the role of DCE magnetic resonance imaging has evolved in the field of perfusion imaging, and several groups have used it in evaluating the perfusion of benign and malignant pancreatic lesions (10, 26–28). Nevertheless, [^{15}O]H_2O PET has been studied more extensively than either DCE-CT or magnetic resonance imaging, and is regarded by some authors as a gold standard in perfusion imaging (15). As previously shown (13, 14), it is a reproducible and reliable method for the quantification of BF in tumor and other tissues such as brain and heart. In addition, CT combined with PET studies has provided the added benefit of precise anatomic localization, the lack of which was often used as an argument against PET in studies of inaccessible abdominal organs like the pancreas. Recent developments have also enabled the extraction of the input curves directly from the images making the procedure

Table 1. BF and FDG SUV_{max} values for normal pancreas, benign lesions, and malignant lesions as well as values for the nontumoral part of the pancreas in their respective patient groups

	Normal pancreas	Benign lesions		Malignant lesions	
		Lesion	Nontumoral part	Lesion	Nontumoral part
BF(mL/min/dL)	113.8 ± 48.2	59.0 ± 26.7	87.5 ± 32.7	45.7 ± 18.2	59.6 ± 40.8
FDG (SUV_{max})	2.6 ± 1.3	2.9 ± 1.0	1.8 ± 0.4	8.0 ± 4.9	2.4 ± 1.4

Table 2. BF, [^{18}F]FDG uptake, and survival of patients with malignant pancreatic lesion

Patient no.	Gender	Age	BF (mL/min/dL)	FDG (SUV_{max})	FDG/BF ratio	Size of tumor (cm)	pTNM/cTNM	Survival (mo)	Therapy (duration mo)
1	F	68	28.9	6.5	0.23	4.7	T4N1bM0	3	No resection/no oncologic treatments
2	F	69	34.8	9.8	0.28	5.0	T3-4NXM1	8	No resection/G (6)
3	M	64	13.2	7.6	0.58	7.5	T4NXM0	3	No resection/G (0.5)
4	F	59	80.6	4.9	0.06	3.0	Insufficient	20*	No resection/G + radiotherapy (7)
5	M	62	29.1	4.1	0.14	6.5	No histology	19*	No resection/G (10)
6	F	74	45.4	8.5	0.19	3.5	T2-3N1M0	6	R1 resection/G (2) + capecitabine
7	F	69	48.9	20.6	0.42	3.5	TXNXM1	5	No resection/reduced G (1)
8	F	67	62.5	5.9	0.09	2.5	Insufficient	14*	No resection/G (12)
9	M	77	53.9	10.8	0.20	5.0	T2-3N1M0	13*	R0 resection/G (8)
10	M	56	51.7	7.8	0.15	8.0	High-grade NET	23*	No resection/somatostatin-analogue (13) Carboplatin/etoposide + streptozocin/5-fluorouracil
11	M	76	53.6	1.6	0.03	2.8	Low-grade NET	PO†	—

Abbreviations: G; gemcitabine; pTNM, pathologic TNM classification; cTNM, clinical TNM classification; SUV_{max}, maximal SUV.
*Alive at closeout.
†Died postoperatively.

more patient-friendly compared with previously used invasive arterial blood sampling (20). This new noninvasive technique has been found to be suitable for routine clinical applications (20) and the findings of pancreatic tumor BF obtained in our study are in line with some of the previous studies of BF in abdominal tumors with [^{15}O]H_2O PET (29). Also, results from the normal pancreas seem to be in line with BF measurements obtained in some other highly perfused abdominal organs such as the spleen (29). The higher uptake of [^{18}F]FDG in malignant tumors compared with benign lesions and normal pancreas is well established and is also seen in the current study.

Relative to other techniques, there are some advantages in measuring tumor perfusion using [^{15}O]H_2O PET. First, PET is currently the most quantitative and best validated method with applications in several tissue and tumor types. An additional advantage of PET imaging is the possibility to concurrently measure metabolic activity using [^{18}F]FDG. Studies on the relationship between metabolism of tumors and their BF have provided quite variable results. Some of the studies were not able to show any correlation between these two variables (23), whereas others found a positive (30) or a negative (31) relationship, depending on tumor type and grade. In the current study, we were not able to show any correlation between these two variables. The diverse findings in different tumor types and sizes reflect the heterogeneity of malignant tissues and also the limited specificity of [^{18}F]FDG to depict neoplastic transformation.

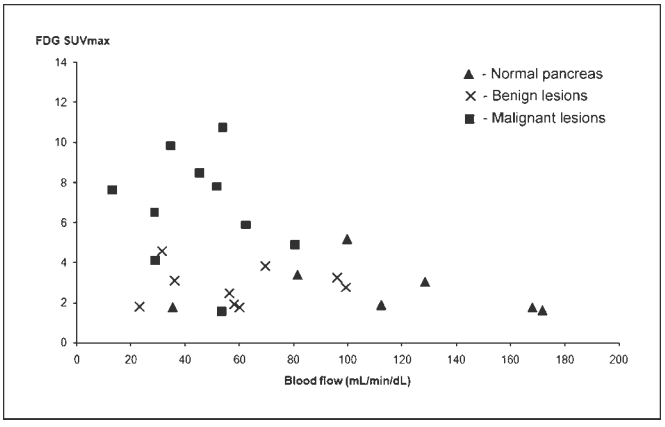

Fig. 3. The relationship between uptake of [^{18}F]FDG and BF for individual patients presenting with malignant lesions (*squares*), benign lesions (*crosses*), and normal pancreas (*triangles*).

Recently, several studies have combined findings on metabolic activity and perfusion to show their effect for prognosis in different types of cancer. Mankoff et al. (32) have described, in patients with breast cancer, the importance of the relationship between BF and metabolic activity of the tumor for treatment outcome. Recently, Groves et al. (33) showed that combining [^{18}F]FDG PET and perfusion measurement helps to predict the histologic grade of breast tumors. In accordance with this, Hermans et al. (34) reported that high glucose metabolism and low vascularity measured by [^{18}F]FDG PET and DCE-CT, respectively, predicted poor local control in head and neck cancer. Our results provide new evidence that pancreatic tumors with high metabolic activity and relatively low BF are aggressive and might be more refractory to treatment than those with higher perfusion. We suggest that high metabolic activity combined with low BF indicates the adaptation of tumors to a hypoxic microenvironment. Hypoxia, in turn, has been shown to be an important factor of selection in the development of aggressive phenotype (35). This is also shown by differential regional distribution of areas of high perfusion, high [^{18}F]FDG uptake, and high SUV/BF ratio within the tumor (Fig. 1), with areas of overlap in which the ratio is high as potential targets for hypoxia-directed radiotherapy. In addition to its prognostic value, our study showed that the SUV/BF ratio could provide a potentially useful tool for differentiating benign pancreatic dysfunction and normal pancreas, which otherwise show substantial overlap in uptake of [^{18}F]FDG.

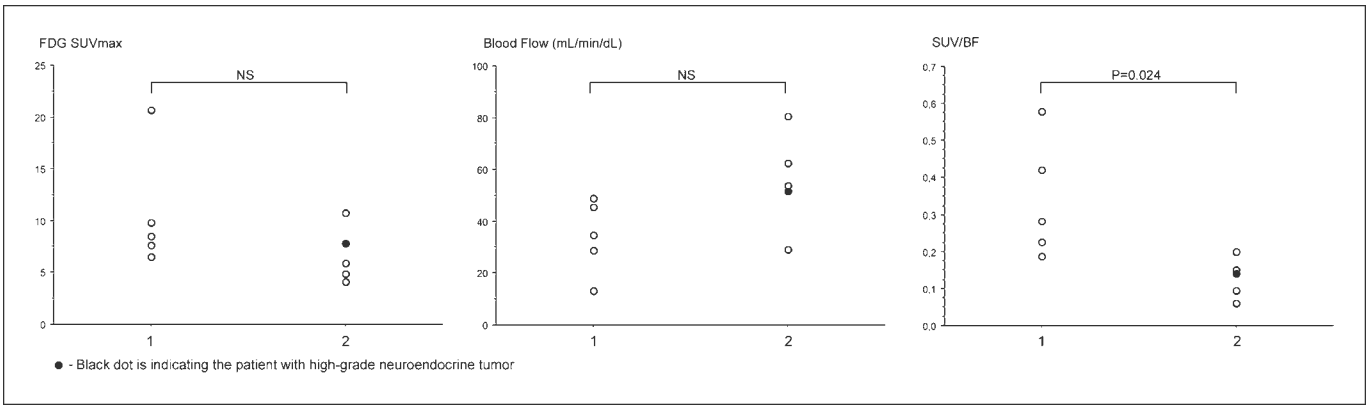

Fig. 4. [^{18}F]FDG SUV_{max}, BF, and the SUV/BF ratio in patients with pancreatic adenocarcinoma that had died (*group 1*) and those still alive at the time of analysis (*group 2*).

Common to all studies applying diverse methodologies is the observation that perfusion in normal pancreas is higher than in pancreatic tumors. An early CT study investigating the vascularity of pancreatic lesions showed that malignant lesions are hypovascular compared with normal pancreas (36). We observed that BF in benign lesions is significantly reduced compared with normal pancreas. However, benign lesions do not seem to have a similar detrimental effect on the BF of the nontumoral parts of the pancreas as malignant lesions do. As first reported by Kubo et al. (11), this reduction seems to be present only in the case of lesions located in the head of the pancreas as confirmed by our findings. This finding might be explained by the fact that tumors located in the head of the pancreas could cause obstruction of the pancreatic duct, followed by formation of fibrotic tissue with low BF in the body-tail region of the pancreas.

Because some variables related to BF have been shown to correlate with microvascular density (37), the use of drugs targeting angiogenesis could be optimized by pretreatment measurement of BF. Both BF and vascularization of tumors vary strongly, and therefore, poor selection of patients might also explain why many clinical trials have failed to show any significant benefit of antiangiogenic therapies in the case of pancreatic malignancy (38). Recently Jain et al. reported that when antiangiogenic therapy is given, tumor vessel permeability and subsequently peritumoral edema decrease. These lead to improvement in effectiveness of tumor perfusion in a process called vessel normalization (39). Other authors have also suggested that normalizing the vasculature of the tumor might improve the response to oncologic therapy (40).

Among the limitations of our study are the small sample size and heterogeneous group of patients with malignant lesions, including two patients with NETs. It is well-known that NETs have a totally different biology and better prognosis compared with pancreatic adenocarcinoma. We included only one patient with high-grade NET in the survival analysis because the second patient with low-grade NET died from postoperative complications after imaging (Fig. 4). As observed in former studies, especially less aggressive forms of NETs show a lower uptake of [^{18}F]FDG and might not be detected on [^{18}F]FDG PET/CT (41). The lowest SUV_{max} of the malignant lesions in the current study (1.6) was indeed observed in a low-grade NET. Additionally, it has been shown that hyperglycemia (42, 43) affects the uptake of [^{18}F]FDG. In spite of the requirement of a 6-hour fast, we found a significantly higher glucose concentration in patients with pancreatic malignancy compared with other patients. As already suggested by others (44, 45), we therefore consider the normalization of [^{18}F]FDG SUVs to GlcP levels to be of particular importance when using [^{18}F]FDG SUVs to quantify the metabolic activity of malignant and benign pancreatic lesions. This might not be needed in purely diagnostic imaging but may be helpful if serial imaging is done to monitor treatment effects.

For the purposed of this study, we decided to use a fixed small-size ROI for a comparison between regional perfusion and metabolism. This was a pragmatic decision and necessary to limit errors associated with organ movement and transfer of ROIs from one image set to another in which differential analytic software was applied. We underline that the ROI was smaller than the smallest tumor and that the results would not have been different even if SUV_{max} was used instead of SUV_{mean} as shown by our supplementary online data.

Conclusion

The differences in BF and its relationship to metabolic activity both in pathologic pancreatic lesions and normal pancreas have been evaluated for the first time using combined [^{15}O]H_2O and [^{18}F]FDG PET/CT. We found both malignant and benign lesions to be associated with decreased perfusion and, in patients with malignant disease, a high ratio of metabolism to BF seemed to predict poor survival. Our preliminary findings in this study, with a limited number of patients, may shed light on the general resistance of pancreatic cancer to oncologic treatments. Finally, we suggest the implementation of combined imaging of perfusion and metabolism in pretreatment evaluation in clinical trials in which antiangiogenic targeting is planned.

Disclosure of Potential Conflicts of Interest

No potential conflicts of interest were disclosed.

Acknowledgments

The authors thank the staff of the Turku Cyclotron and the Radiochemistry Laboratory for technical support and advice, and the staff of the Turku PET Center for excellent help in imaging patients. We also thank Irina Lisinen, MsC, for consultation on the statistical analyses, and Kalle Alanen, MD, for histopathologic analysis.

References

1. Jemal A, Siegel R, Ward E, Murray T, Xu J, Thun MJ. Cancer statistics, 2007. CA Cancer J Clin 2007;57:43–66.
2. Li D, Xie K, Wolff R, Abbruzzese JL. Pancreatic cancer. Lancet 2004;363:1049–57.
3. Twombly R. Adjuvant chemoradiation for pancreatic cancer: few good data, much debate. J Natl Cancer Inst 2008;100:1670–1.
4. Reuter SR, Redman HC, Bookstein JJ. Differential problems in the angiographic diagnosis of carcinoma of the pancreas. Radiology 1970;96:93–9.
5. Lang SA, Schachtschneider P, Moser C, et al. Dual targeting of Raf and VEGF receptor 2 reduces growth and metastasis of pancreatic cancer through direct effects on tumor cells, endothelial cells, and pericytes. Mol Cancer Ther 2008;7:3509–18.
6. Longo R, Cacciamani F, Naso G, Gasparini G. Pancreatic cancer: from molecular signature to target therapy. Crit Rev Oncol Hematol 2008;68: 197–211.
7. Miles KA, Hayball MP, Dixon AK. Measurement of human pancreatic perfusion using dynamic computed tomography with perfusion imaging. Br J Radiol 1995;68:471–5.
8. Bize PE, Platon A, Becker CD, Poletti PA. Perfusion measurement in acute pancreatitis using dynamic perfusion MDCT. AJR Am J Roentgenol 2006;186:114–8.
9. Sofuni A, Iijima H, Moriyasu F, et al. Differential diagnosis of pancreatic tumors using ultrasound contrast imaging. J Gastroenterol 2005;40:518–25.
10. Bali MA, Metens T, Denolin V, De M, Deviere V, Matos J. Pancreatic perfusion: noninvasive quantitative assessment with dynamic contrast-enhanced MR imaging without and with secretin stimulation in healthy volunteers—initial results. Radiology 2008;247:115–21.
11. Kubo S, Yamamoto K, Magata Y, et al. Assessment of pancreatic blood flow with positron emission tomography and oxygen-15 water. Ann Nucl Med 1991;5:133–8.
12. Anderson H, Price P. Clinical measurement of blood flow in tumours using positron emission tomography: a review. Nucl Med Commun 2002;23:131–8.
13. de Langen AJ, Lubberink M, Boellaard R, et al. Reproducibility of tumor perfusion measurements using 15O-labeled water and PET. J Nucl Med 2008;49:1763–8.
14. Lodge MA, Jacene HA, Pili R, Wahl RL. Reproducibility of tumor blood flow quantification with 15O-water PET. J Nucl Med 2008;49:1620–7.
15. Rajendran JG. Positron emission tomography imaging of blood flow and hypoxia in tumors. In: Mankoff DA, editor. Cancer drug discovery and development *in vivo* imaging of cancer therapy. Totowa (NJ): Humana Press, Inc.; 2008, p. 47–71.
16. Miles KA, Williams RE. Warburg revisited: imaging tumour blood flow and metabolism. Cancer Imaging 2008;8:81–6.
17. Teras M, Tolvanen T, Johansson JJ, Williams JJ, Knuuti J. Performance of the new generation of whole-body PET/CT scanners: Discovery STE and Discovery VCT. Eur J Nucl Med Mol Imaging 2007;34:1683–92.
18. Komar G, Seppanen M, Eskola O, et al. 18F-EF5: a new PET tracer for imaging hypoxia in head and neck cancer. J Nucl Med 2008;49: 1944–51.
19. Blomqvist G. On the construction of functional maps in positron emission tomography. J Cereb Blood Flow Metab 1984;4:629–32.
20. Liukko KE, Oikonen V, Tolvanen T, et al. Noninvasive estimation of subcutaneous and visceral adipose tissue blood flow by using 15OH2O PET with image derived input functions. Open Med Imaging J 2007;1:7–13.
21. Boellaard R, Oyen WJ, Hoekstra CJ, et al. The Netherlands protocol for standardisation and quantification of FDG whole body PET studies in multi-centre trials. Eur J Nucl Med Mol Imaging 2008;35:2320–33.
22. Nalluri SR, Chu D, Keresztes R, Zhu X, Wu S. Risk of venous thromboembolism with the angiogenesis inhibitor bevacizumab in cancer patients: a meta-analysis. JAMA 2008;300:2277–85.
23. Hoekstra CJ, Stroobants SG, Hoekstra OS, Smit EF, Vansteenkiste JF, Lammertsma AA. Measurement of perfusion in stage IIIA-N2 non-small cell lung cancer using H(2)(15)O and positron emission tomography. Clin Cancer Res 2002;8:2109–15.
24. D'Onofrio M, Martone E, Malago R, et al. Contrast-enhanced ultrasonography of the pancreas. JOP 2007;8:71–6.
25. Park MS, Klotz E, Kim MJ, et al. Perfusion CT: noninvasive surrogate marker for stratification of pancreatic cancer response to concurrent chemo- and radiation therapy. Radiology 2009;250:110–7.
26. Tajima Y, Matsuzaki S, Furui J, Isomoto I, Hayashi K, Kanematsu T. Use of the time-signal intensity curve from dynamic magnetic resonance imaging to evaluate remnant pancreatic fibrosis after pancreaticojejunostomy in patients undergoing pancreaticoduodenectomy. Br J Surg 2004;91:595–600.
27. Coenegrachts K, Van Steenbergen W, De Keyzer F, et al. Dynamic contrast-enhanced MRI of the pancreas: initial results in healthy volunteers and patients with chronic pancreatitis. J Magn Reson Imaging 2004;20:990–7.
28. Lee SS, Byun JH, Park BJ, et al. Quantitative analysis of diffusion-weighted magnetic resonance imaging of the pancreas: usefulness in characterizing solid pancreatic masses. J Magn Reson Imaging 2008;28:928–36.
29. Wells P, Jones T, Price P. Assessment of inter- and intrapatient variability in C15O2 positron emission tomography measurements of blood flow in patients with intra-abdominal cancers. Clin Cancer Res 2003;9:6350–6.
30. Zasadny KR, Tatsumi M, Wahl RL. FDG metabolism and uptake versus blood flow in women with untreated primary breast cancers. Eur J Nucl Med Mol Imaging 2003;30:274–80.
31. Hirasawa H, Tsushima Y, Hirasawa S, et al. Perfusion CT of breast carcinoma: arterial perfusion of nonscirrhous carcinoma was higher than that of scirrhous carcinoma. Acad Radiol 2007;14:547–52.
32. Mankoff DA, Dunnwald LK, Gralow JR, et al. Blood flow and metabolism in locally advanced breast cancer: relationship to response to therapy. J Nucl Med 2002;43:500–9.
33. Groves AM, Wishart GC, Shastry M, et al. Metabolic-flow relationships in primary breast cancer: feasibility of combined PET/dynamic contrast-enhanced CT. Eur J Nucl Med Mol Imaging 2009;36:416–21.
34. Hermans R, Meijerink M, Van den BW, Rijnders A, Weltens C, Lambin P. Tumor perfusion rate determined noninvasively by dynamic computed tomography predicts outcome in head-and-neck cancer after radiotherapy. Int J Radiat Oncol Biol Phys 2003;57:1351–6.
35. Smalley KS, Brafford PA, Herlyn M. Selective evolutionary pressure from the tissue microenvironment drives tumor progression. Semin Cancer Biol 2005;15:451–9.
36. Hosoki T. Dynamic CT of pancreatic tumors. AJR Am J Roentgenol 1983;140:959–65.
37. Folkman J. Role of angiogenesis in tumor growth and metastasis. Semin Oncol 2002;29: 15–8.
38. Kindler HL. A double-blind, placebo-controlled, randomized phase III trial of gemsitabine (G) plus bevacizumab versus gemsitabine plus placebo (P) in patients with advanced pancreatic cancer (PC): a preliminary analysis of Cancer and Leukemia Group B (CALGB). In: Niedzwiecki D, editor. 25 no. 18S ed. 2007.
39. Jain RK, Tong RT, Munn LL. Effect of vascular normalization by antiangiogenic therapy on interstitial hypertension, peritumor edema, and lymphatic metastasis: insights from a mathematical model. Cancer Res 2007;67: 2729–35.
40. Stockmann C, Doedens A, Weidemann A, et al. Deletion of vascular endothelial growth factor in myeloid cells accelerates tumorigenesis. Nature 2008;456:814–8.
41. Adams S, Baum R, Rink T, Schumm-Drager PM, Usadel KH, Hor G. Limited value of fluorine-18 fluorodeoxyglucose positron emission tomography for the imaging of neuroendocrine tumours. Eur J Nucl Med 1998;25:79–83.
42. Zimny M, Buell U, Diederichs CG, Reske SN. False-positive FDG PET in patients with pancreatic masses: an issue of proper patient selection? Eur J Nucl Med 1998;25:1352.
43. Delbeke D, Rose DM, Chapman WC, et al. Optimal interpretation of FDG PET in the diagnosis, staging and management of pancreatic carcinoma. J Nucl Med 1999;40:1784–91.
44. Kroep JR, Van Groeningen CJ, Cuesta MA, et al. Positron emission tomography using 2-deoxy-2-[18F]-fluoro-D-glucose for response monitoring in locally advanced gastroesophageal cancer: a comparison of different analytical methods. Mol Imaging Biol 2003;5: 337–46.
45. Krak NC, Hoekstra OS, Lammertsma AA. Measuring response to chemotherapy in locally advanced breast cancer: methodological considerations. Eur J Nucl Med Mol Imaging 2004;31:103–11.